

## Research Article

# Effect of irradiation with heavy $\text{Xe}^{22+}$ ions with energies of 165–230 MeV on change in optical characteristics of $\text{ZrO}_2$ ceramic

I.A. Ivanov<sup>a,b</sup>, M. Alin<sup>a</sup>, M.V. Koloberdin<sup>b</sup>, A. Sapar<sup>a,b</sup>, A.E. Kurakhmedov<sup>b</sup>, A. L. Kozlovskiy<sup>a,b,\*</sup>, M.V. Zdorovets<sup>a,b,c</sup>, V.V. Uglov<sup>d</sup>

<sup>a</sup> L.N. Gumilyov Eurasian National University, Nur-Sultan, Kazakhstan

<sup>b</sup> The Institute of Nuclear Physics of Republic of Kazakhstan, Almaty, Kazakhstan

<sup>c</sup> Ural Federal University, Yekaterinburg, Russia

<sup>d</sup> Belarusian State University, Minsk, Belarus



## ARTICLE INFO

## Keywords:

Swift heavy ion  
Optical properties  
Absorbance  
Defects  
 $\text{ZrO}_2$  ceramic  
Irradiation

## ABSTRACT

The aim of this work is to study the effect of irradiation with heavy  $\text{Xe}^{22+}$  ions with energies of 165 MeV, 200 MeV, and 230 MeV on the change in the optical properties of  $\text{ZrO}_2$  ceramic. The choice of ion energies, as well as irradiation fluences of  $10^{13}$ – $10^{14}$  ion/cm<sup>2</sup>, is primarily due to the possibility of simulating radiation damage in ceramics that occurs when overlapping damaged areas in the material, comparable to damage from fission fragments of uranium nuclei in an atomic reactor. Using UV–Vis spectroscopy methods, changes in the throughput of ceramics were evaluated depending on the irradiation fluence and the energy of incident ions. It was found that a change in the irradiation conditions leads to the formation of irradiation-induced defects with an energy of 2.4–2.45 eV in the structure, the concentration of which increases with the irradiation dose. Changes in the band gap and refractive index depending on irradiation fluence and incident ions energy indicate a change in the electronic and optical density of ceramics, as well as the formation of additional absorbing centers in the structure.

## 1. Introduction

Today, oxide dielectric ceramics or nanostructured oxide ceramics are one of the promising classes of materials for a wide range of practical applications. Interest in them is due to their physical and chemical properties, as well as high resistance to external influences, as well as various modifications, which open up broad prospects for their application in various industries, including energy [1–8]. At the same time, special attention among researchers is paid to the study of both the methods of obtaining oxide ceramics and the study of the effect of external influences, corrosion processes, and radiation damage on them.

One of the important directions in modern materials science and energy is the study of the behavior of structural and optical changes in dielectric ceramics arising under external influences, such as corrosion, exposure to aggressive media, radiation exposure [9–14]. The study of such processes plays a highly important role in determination of performance characteristics of materials, as well as their resistance to external influences. At the same time, both theoretical research and experimental data are important in these studies, which allow

developing not only the foundations of studying the properties of materials and the dynamics of their change, but also to obtain practical knowledge necessary for the design and application of materials in industry [15–19].

The most important area of research in the study of the influence of external factors is the study of the radiation damage effect on physico-chemical properties of dielectric ceramics, which arise when they interact with ionizing radiation [20,21]. In case of irradiation of structural materials or ceramics with different types of ionizing radiation, processes of radiation interaction with crystalline structure of materials have multi-stage and complex character, including primary and secondary processes of radiation interaction with matter [22,23]. The final stage of primary processes is ionization and the formation of primary knocked-out atoms, which entail a change in electron density in the material. Secondary processes, in turn, lead to the formation of point defects, vacancies, and disordering regions at high irradiation fluences. It is important to note here that the final evolution of both primary and secondary processes has a direct dependence on the irradiation fluences and the formed defective regions [24–26]. For example, with small

\* Corresponding author. L.N. Gumilyov Eurasian National University, Nur-Sultan, Kazakhstan.

E-mail address: [kozlovskiy.a@inp.kz](mailto:kozlovskiy.a@inp.kz) (A.L. Kozlovskiy).

irradiation fluences, defective regions in dielectric ceramics are isolated from each other, resulting in the formation of single defects and a low disordering degree, which in most cases do not significantly affect the change in material properties. At high irradiation fluences, which are characterized by the formation of defect overlap regions, these disordering regions and point defects are not isolated from each other and, therefore, make a collective contribution to the change in the properties of materials, which can be catastrophic in some cases. It should be noted that, according to various estimates, the boundary of defect regions overlapping onset varies from  $10^{12}$  to  $10^{14}$  ion/cm<sup>2</sup>, depending on the type of incident ions and their energies [27,28]. In turn, depending on the class of materials, the final evolution of radiation damage also has significant differences, which leads to the inadmissibility of applying a unified theory to describe all the observed effects and gives rise to a large number of different theoretical interpretations of radiation defects in materials. In particular, for ceramics, the theory most commonly used to describe radiation damage is the theory of the formation of so-called thermal bursts or thermal peaks arising along the trajectory of an incident particle, which are accompanied by the appearance of local temperature gradients comparable to the plasma temperature [29–31]. The formation of such local regions results in a large number of small point defects capable of making significant changes in the properties of materials, up to the formation of radiation damage, called latent tracks or disordering regions [32,33]. Moreover, if for metals the occurrence and subsequent evolution of radiation damage is well described and has a large number of experimental evidence of the proposed theoretical research, then for ceramics, in particular zirconia, such data are quite small, despite the great interest in this class of ceramics, both from a fundamental and practical point of view.

As is known, ceramics based on zirconium dioxide are one of the promising classes of ionic conductors that have found wide application in various technological applications, as well as in nuclear power [34–38]. As is known from previous studies, ceramics based on zirconium oxide, as well as their various modifications, have unique optical properties, which make it possible to use them in a wide range of practical applications [39–42]. In this case, the previously established processes of phase transformations [43] under the action of irradiation in ZrO<sub>2</sub> ceramic open up a large number of questions concerning the effect of irradiation not only on the structural properties of ceramics, but also on optical characteristics, since this type of ceramics has great potential for use as a basis for optical devices capable of operating in conditions of increased radiation background, including in the core of nuclear reactors.

Based on the foregoing, the aim of this work is to study the effect of irradiation with heavy ions Xe<sup>22+</sup> with energies of 165 MeV, 200 MeV, and 230 MeV on the change in the optical properties of ZrO<sub>2</sub> ceramic. The choice of ion energies, as well as radiation fluences of  $10^{13}$ – $10^{14}$  ion/cm<sup>2</sup>, is primarily due to the possibility of simulating radiation damage in ceramics that occurs when overlapping damaged areas in the material, comparable to damage from fission fragments of uranium nuclei in an atomic reactor.

## 2. Experimental part

The initial samples were polycrystalline ZrO<sub>2</sub> ceramics with a tetragonal crystal lattice and spatial system P42/nmc (137).

The initial polycrystalline ZrO<sub>2</sub> ceramic samples were irradiated with heavy Xe<sup>22+</sup> ions with energies of 165 MeV, 200 MeV, and 230 MeV and fluences of  $10^{13}$ – $10^{14}$  ion/cm<sup>2</sup>. The choice of radiation doses is due to the possibility of simulating the effects of radiation damage and the initialization of gas swelling processes under irradiation with uranium fission fragments. According to calculated data, the concentration of implanted Xe<sup>22+</sup> ions in the structure of ceramics is 0.001–0.01 at.%. In view of the large atomic radius and low mobility of implanted Xe<sup>22+</sup> ions, the final stage of evolution is the formation of gas-filled bubbles in the near-surface layer. The formation of such bubbles leads to a decrease

in mechanical, heat-conducting, strength properties, as well as optical characteristics.

The irradiation of samples was carried out on a DC-60 heavy ion accelerator, on the third channel designed to simulate radiation damage by various types of ions in a wide energy range. The samples were placed in a special target holder cooled with water in order to avoid heating the samples during irradiation. The temperature of the samples during irradiation was no more than 50–70 °C.

Determination of the radiation effect and the consequences of radiation damage on the change in optical properties, as well as the change in optical and electron density were carried out using optical UV–Vis spectroscopy, by taking UV–Vis spectra in the wavelength range from 300 to 800 nm, with a step of 1 nm.

Determination of the induced absorption value was carried out by logarithm of the ratio of the transmission spectra. The absorption value characterizing the change in optical and electron density was estimated by changing the transmission spectra and the shift of the fundamental absorption edge.

The determination of the band gap and refractive index was carried out by making Tauc plots and subsequent analysis.

## 3. Results and discussion

Fig. 1 shows the results of measuring the optical transmission spectra of the studied ZrO<sub>2</sub> ceramic depending on the energy and fluence of incident ions. In this section, the UV–Vis spectra are grouped as a dependence of the increase in the radiation dose at one ion energy. This grouping is due to the need to show changes in optical transmission spectra depending on an increase in radiation damage degree at the same energy of incident ions. The initial transmission spectrum of ZrO<sub>2</sub> ceramic is characterized by a fundamental absorption edge in the region of 320–350 nm, as well as high transmission rates in a wide wavelength range. The main nature of the change in optical properties depending on the radiation dose is primarily associated with a shift in the fundamental absorption edge, as well as a sharp drop in the transmission value in the region of 400–600 nm.

As can be seen from the data presented, a decrease in the transmission value in the range of 400–600 nm may be due to the formation of nanostructured inclusions or the fragmentation of grains with a metallic type of conductivity. Similar effects were observed when ZrO<sub>2</sub> ceramic were irradiated with ion irradiation [43–45]. Thus, the authors of these works have shown that when irradiated with low-energy ions with a large irradiation fluence, nanoinclusions are formed in the near-surface irradiated layer, which lead to the appearance of additional absorption centers and thereby reduce the transmission in this region. The formation of such inclusions, as shown by the authors of [43–45], leads to an increase in the absorption of light in this wavelength range. The very formation of such inclusions can be associated with the processes of knocking out zirconium ions from the sites of the crystal lattice and their subsequent coagulation, as well as rearrangement of the crystal lattice and its deformation. In this case, an increase in the energy of incident ions leads to more intense absorption in this region, which indicates an increase in the concentration of these absorbing centers and defects in the structure.

All obtained transmission variation dependences can be divided into two groups. The first group of changes is associated with an increase in irradiation fluence and is characterized by dependencies of a decrease in transmission with an increase in the irradiation fluence and, as is known, the concentration of radiation damage areas. In the case of energies of incident ions of 165 MeV, an increase in irradiation fluence from  $10^{13}$  to  $5 \times 10^{13}$  ion/cm<sup>2</sup> leads to a reduction in transmission by 51.3% and 54.5%, respectively compared to the initial value. At the same time, the increase in fluence from  $10^{13}$  to  $5 \times 10^{13}$  ion/cm<sup>2</sup> leads to a decrease in transmission by only 3.2%, while a further increase in irradiation fluence up to  $10^{14}$  ion/cm<sup>2</sup> leads to a decrease in the transmission by 60.9% compared to the initial value of 9.6% compared with the initial value

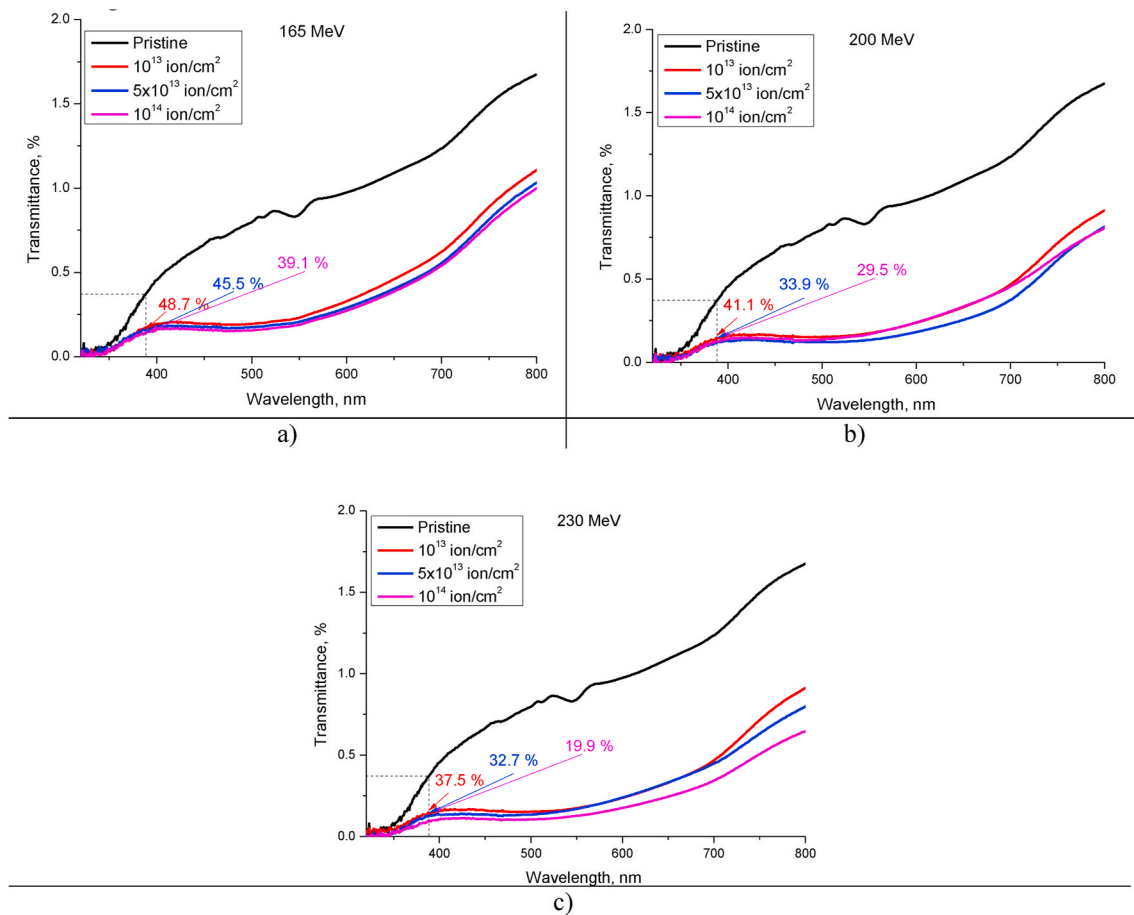


Fig. 1. UV-Vis transmission spectra of ZrO<sub>2</sub> ceramic before and after irradiation with heavy Xe<sup>22+</sup> ions with various energies: a) 165 MeV; b) 200 MeV; c) 230 MeV.

and 9.6% and 6.4% compared to the similar transmission values for samples irradiated with doses of  $10^{13}$  to  $5 \times 10^{13}$  ion/cm<sup>2</sup>.

For samples irradiated with 200 MeV ions, the transmission decrease is more pronounced and is 58.9%, 66.1% and 70.5% for irradiation fluences  $10^{13}$ ,  $5 \times 10^{13}$  and  $10^{14}$  ion/cm<sup>2</sup>, respectively. For samples irradiated with 230 MeV ions, a further decrease of 62.5%, 67.3% and 80.1% for irradiation fluences  $10^{13}$ ,  $5 \times 10^{13}$  and  $10^{14}$  ion/cm<sup>2</sup>, respectively, is observed.

Such a decrease in transmittance is primarily due to large energy losses of the incident ions, which lead to an increase in the concentration of formed point defects, vacancies and primarily knocked out atoms, as well as an increase in the radius of the damage region. An increase in radiation damage areas along ion trajectories in the material while increasing the energy of the incident ions leads to an increase in overlapping degree of such regions and, therefore, more intense mixing of the formed point defects and vacancies. At the same time, an increase in irradiation fluence from  $5 \times 10^{13}$  ion/cm<sup>2</sup> to  $10^{14}$  ion/cm<sup>2</sup>, according to estimates given in the monograph [46], can lead to an increase in defective regions overlapping degree up to 100–1000 times. At the same time, according to Ref. [47] for ions with energies of more than 50 MeV, the predominance of electronic losses in the interaction of incident ions with a substance leads to the occurrence of local ionization, which causes further radiation damage. At the same time, as is known, the oxygen binding energy in the structure of ZrO<sub>2</sub> ceramic is much less than the zirconium binding energy, as a result of which the mobility of oxygen ions is much higher than that of zirconium ions, which leads to the formation of a large number of oxygen vacancies. Knocked out oxygen ions can migrate along the crystal lattice, and slow-moving zirconium ions can form additional defects, attaching electrons to themselves, thereby forming the nanoscale inclusions mentioned in works [43–45].

Such a similar behavior of the change in transmission value in the case of heavy ions is due to the fact that during irradiation, the energy losses of incident particles during elastic and inelastic interactions are several orders of magnitude higher than during low-energy irradiation, as a result of collisions, as well as primarily knocked out atoms in this case are much greater than during low-energy irradiation. It is worth to note that during high-energy irradiation, the interactions of incident ions with electron shells play an important role, which lead to the formation of a large number of knocked out electrons and, consequently, there is a change in the electron density near trajectories of ions in the material. In contrast to metals, for which relaxation processes play a significant role and after irradiation, most of the knocked out electrons return to their original positions, thereby compensating for changes in the electron density, for dielectrics such a process is extremely difficult, which can lead to the formation of regions with depleted or over-saturated electrons. The formation of such areas can lead to a change in the band gap, the results of which are shown in Fig. 2.

The general appearance of the band gap changes is related to the displacement of the fundamental absorption edge into the low energy region, which indicates a change in electron density and the formation of additional defects leading to absorption. Based on the obtained Tauc plots, the band gap and refractive index were determined, the data of which are shown in Table 1.

The determination of the band gap value was carried out using formula (1):

$$\alpha = A(h\nu - E_g)^{1/2}, \quad (1)$$

where  $A$  is a constant and  $h\nu$  is the photon energy.

The refractive index was determined using the following formula (2):

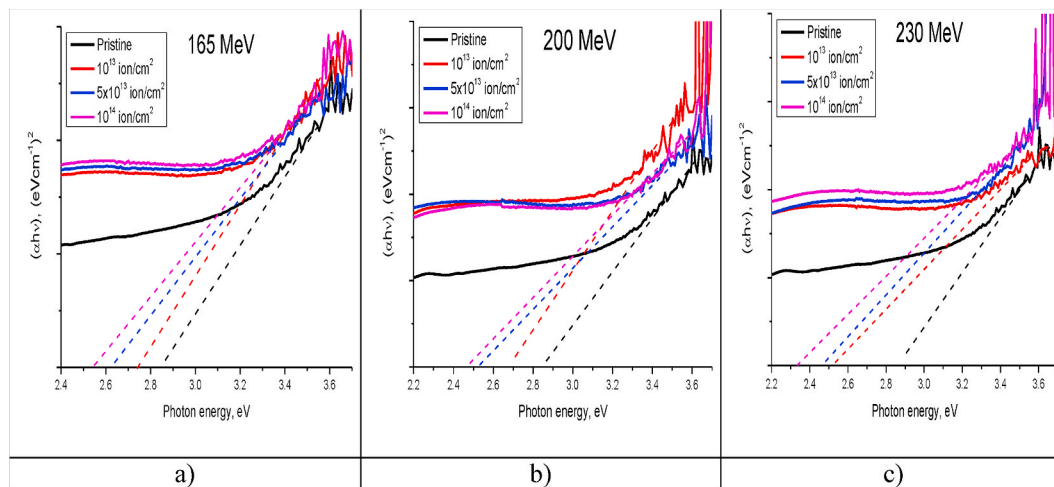


Fig. 2. Tauc plots a) 165 MeV; b) 200 MeV; c) 230 MeV.

Table 1

Data on changes in the values of the band gap and refractive index depending on the radiation dose.

Fluence, ion/cm <sup>2</sup>	Band gap, eV			
	Initial	165 MeV	200 MeV	230 MeV
10 <sup>13</sup>	2.85	2.74	2.68	2.63
5 × 10 <sup>13</sup>		2.62	2.54	2.46
10 <sup>14</sup>		2.55	2.47	2.34
Fluence, ion/cm <sup>2</sup>	Refractive index			
	Initial	165 MeV	200 MeV	230 MeV
10 <sup>13</sup>	2.44	2.47	2.49	2.50
5 × 10 <sup>13</sup>		2.51	2.53	2.56
10 <sup>14</sup>		2.53	2.56	2.60

$$\frac{|(n^{optical})^2 - 1|}{|(n^{optical})^2 + 2|} = 1 - \sqrt{\frac{E_g}{20}}, \quad (2)$$

where  $E_g$  is the band gap.  $\alpha = A(h\nu - E_g)^{1/2}$ ,

According to the obtained data, the largest changes in the band gap and refractive index are observed at large fluences and at maximum energies of incident ions. As mentioned above, such changes may be associated with changes in the optical density of the ceramics, the changes of which are directly dependent on radiation damage concentration and irradiation density. The formation of overlapping regions of damaged areas that occur along the ions movement trajectory in the material leads to the appearance of regions with an anisotropic distribution of electrons. At the same time, an increase in the energy of incident ions and the irradiation fluence leads to both an increase in the overlapping degree and an increase in the electron density distribution anisotropy. As previously shown, for dielectric materials, including polymers and ceramics, high-dose irradiation leads to the formation of crystal and electron anisotropy in the structure, which are expressed in a change in the diffraction maxima intensity with a circular scan of  $\phi = 0-360^\circ$  [48,49], as well as the appearance of additional induced absorption bands, indicating a change in the electron density in the material [50]. Also, changes in the electron density can be associated with induced phase transformations of the t-ZrO<sub>2</sub> → c-ZrO<sub>2</sub> type in the structure of ZrO<sub>2</sub> ceramic under the action of irradiation with heavy ions [43].

An increase in the refractive index, in turn, characterizes an increase in the optical density, which is due to the formation of additional absorbing centers in the near-surface irradiated layer. As a rule, in dielectrics, the change in optical density (absorbance) depending on the irradiation fluence is characterized by a linear dependence, and the

nature of linearity indicates the rate of increase in the concentration of defects and absorbing centers in the irradiated material. Fig. 3a shows the results of change in absorbance depending on the energy of incident ions and irradiation fluence.

As can be seen from the data presented, the obtained dependences of the change in the optical density have are in good agreement with the previously obtained data of linear dependences for irradiated materials. At the same time, an increase in the energy of incident ions from 165 MeV to 200 MeV does not affect the slope of the optical density change line, while irradiation with ions with an energy of 230 MeV leads to a sharp increase in the angle of inclination of the line, which indicates an increase in the defect formation rate in the irradiated material. In turn, an increase in optical density indicates an increase in the concentration of absorbing centers arising from irradiation. Applying a known expression that binds the optical density with the depth of radiation damage caused by irradiation and subsequent formation of defects, the dependence of change in depth of the lower concentration of optical defects caused by irradiation from the radiation dose and the energy of incident ions was constructed. The results of the constructions are presented in Fig. 3b, according to which it can be seen that an increase in both the irradiation fluence and the energy of the incident ions leads to an increase in the thickness of the damaged layer with accumulated defects. An increase in optical density, as well as a layer depth with a modified optical density, can be due not only to radiation damage caused by the ionization processes and the subsequent formation of point and vacancy defects, but also to the formation of additional defects capable of forming additional absorbing centers. The formation of such centers can be associated both with the formed oxygen vacancies, as a result of knocked out oxygen from the crystal lattice nodes, and the formation of T-defects (zirconium ion + electron) arising from the breaking of chemical and crystalline bonds. In turn, the knocked out oxygen ions migrating to the surface create a large number of oxygen vacancies in the structure, and also create a positive charge gradient in the irradiated layer, which is compensated by the knocked out electrons. The charge compensation leads to the filling of a part of the energy levels in the band gap, which leads to its decrease. In this case, the formed T-defects will accumulate near the bottom of the conduction band due to the 4d-states of Zr, which form the valence band.

Fig. 4 shows the results of determining changes in the induced absorption value, which was calculated by logarithm of the ratio of transmission spectra of ceramics in the initial and irradiated state. The difference spectrum in the energy representation reflects the formation of additional absorption bands in ceramics with a maximum of 2.4–2.45 eV, which corresponds to the formation energy of T-defects.

As can be seen from the data presented, an increase in the radiation

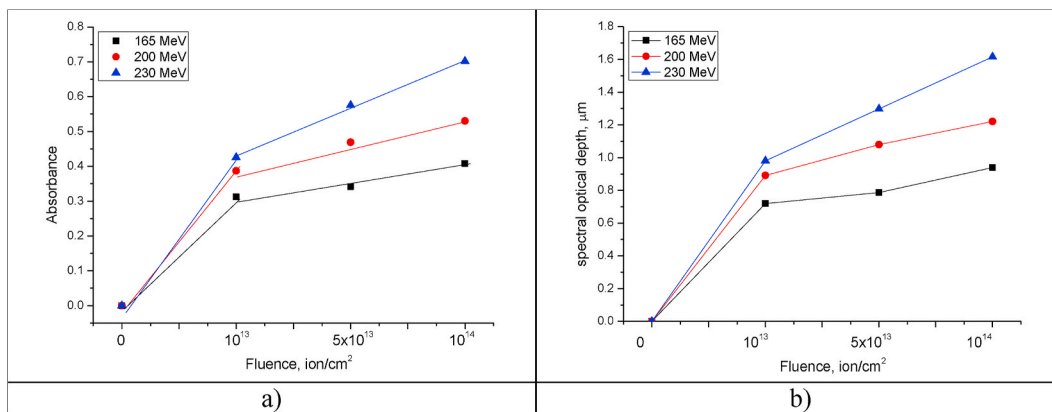


Fig. 3. a) Graph of the change in absorbance depending on irradiation fluence for  $Xe^{22+}$  ions of different energies; b) Graph of the change in optical depth of radiation damage induced by defects.

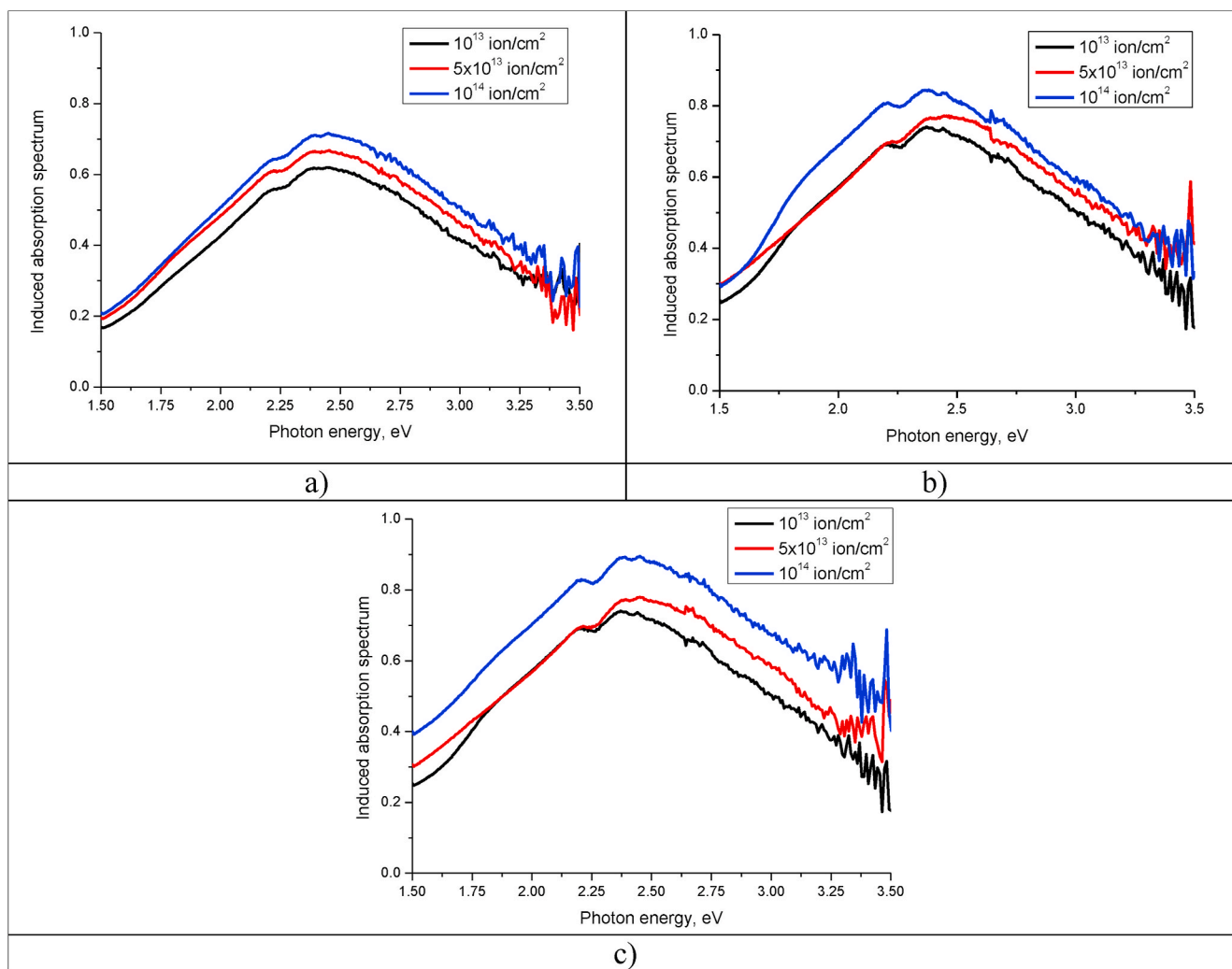


Fig. 4. Graphs of the induced absorption in ceramics after irradiation with  $Xe^{22+}$  ions with different energies: a) 165 MeV; b) 200 MeV; c) 230 MeV.

dose leads to an increase in the induced absorption band intensity, which indicates an increase in the concentration of formed defects. At the same time, an increase in the ion energy to 200 and 230 MeV leads to the formation of double maxima, which indicates the formation of additional C-type defects associated with the formation of zirconium ions with two oxygen vacancies nearby. Evaluation of the induced

absorption spectra maximum values (see Fig. 5) indicates that an increase in the energy of incident ions from 200 to 230 MeV at irradiation doses of  $10^{13}$ - $5 \times 10^{13}$  ion/cm<sup>2</sup> leads to an insignificant increase in the concentration of induced defects, as compared to a similar value obtained from the analysis of the induced absorption spectra intensity of samples irradiated with an ion energy of 165 MeV.

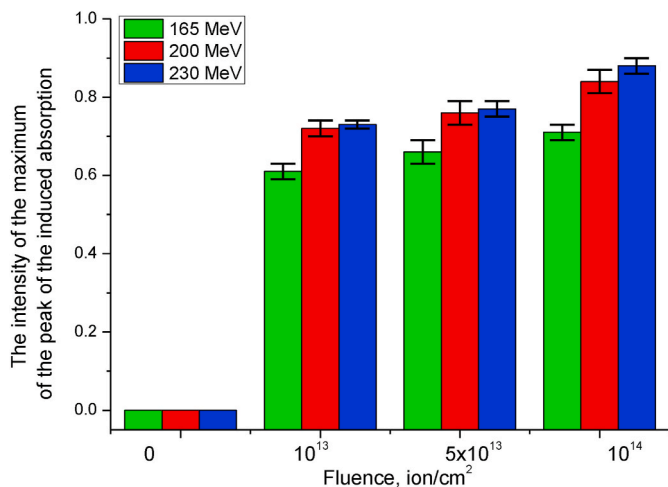


Fig. 5. Diagram of the change in the induced absorption peak maximum, which characterizes the concentration of defects resulting from irradiation.

The dependences of change in transmission spectra shown in Fig. 6, grouped depending on the energy of incident ions at the same irradiation fluence, indicate that an increase in the energy of incident ions by an amount of 30–35 MeV leads to significant differences in the change in transmittance at doses of 10<sup>13</sup>–5x10<sup>13</sup> ion/cm<sup>2</sup>, which range from 1.2 to

7–12% depending on the ion energy, while for samples irradiated at a fluence of 10<sup>14</sup> ion/cm<sup>2</sup>, the average decrease in transmittance is 10% with an increase in the energy of ions. Such differences may be due to a change in the probability of overlapping defective regions, which for fluence 10<sup>13</sup>–5x10<sup>13</sup> ion/cm<sup>2</sup> is 10–50 times the overlap, according to estimates [46], and has a pronounced dependence on the radii of these regions. According to estimates from earlier studies, the radius of this region can vary from 3 to 10 nm depending on the energy of the incident particles. At the same time, the radius of the region with the changed electron density, according to some estimates, can significantly exceed these dimensions, depending on the energy of the particles [51]. While for irradiation fluence of 10<sup>14</sup> ion/cm<sup>2</sup>, this value is much larger, and thus the dependence on the radius of the damaged area becomes not as significant as for small fluences.

#### 4. Conclusion

The paper presents the results of a study of the effect of Xe<sup>22+</sup> heavy ion irradiation on the optical properties of ZrO<sub>2</sub> ceramic. The study of optical characteristics was carried out using the UV–Vis spectroscopy, which allows assessing with high accuracy the change in transmission, band gap, refractive index and induced absorption without destroying the samples. The obtained dependences of changes in optical properties of ZrO<sub>2</sub> ceramic characterize the effect of radiation damage in a wide energy and dose range. During the studies, it was found that an increase in the energy of incident ions by 30–35 MeV leads to significant

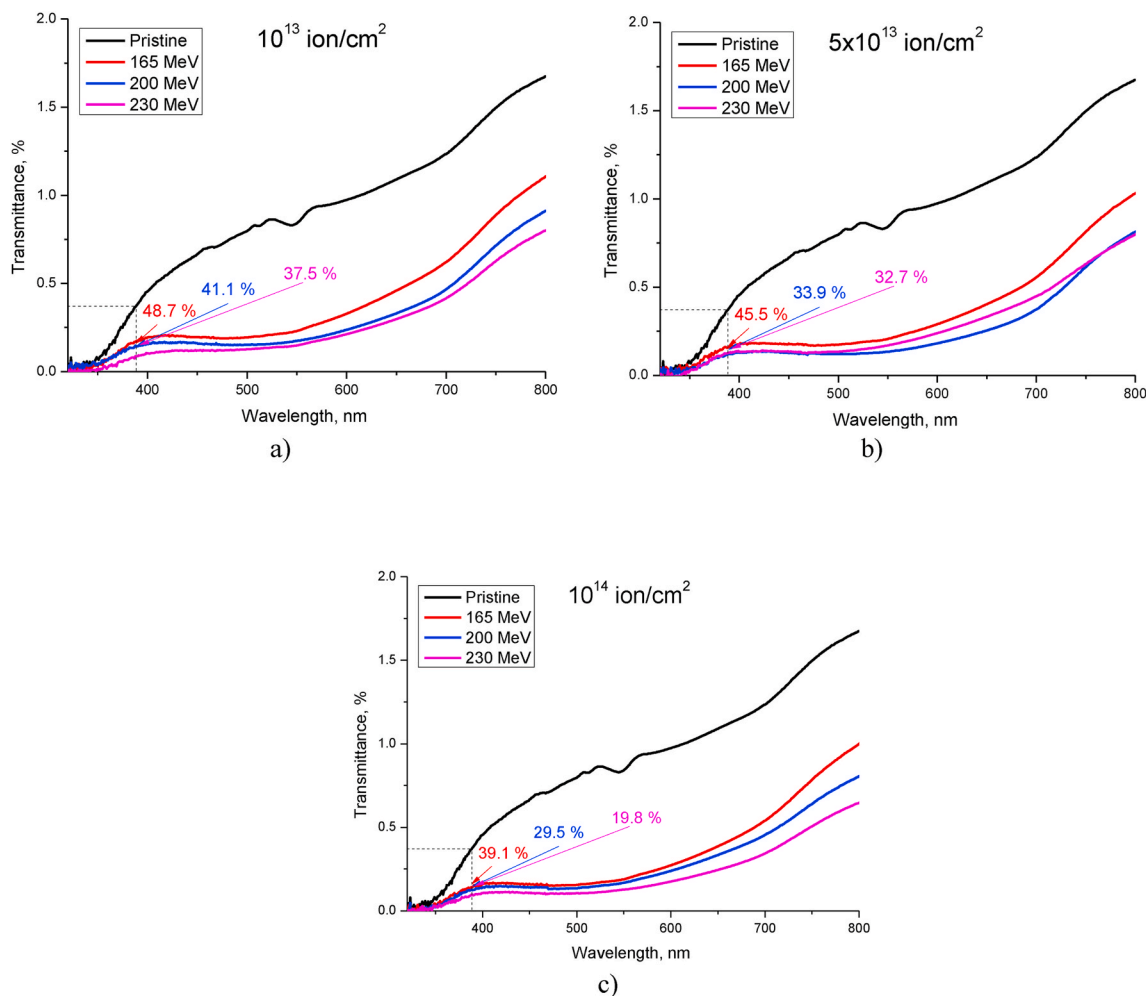


Fig. 6. UV–Vis transmission spectra of ZrO<sub>2</sub> ceramics before and after irradiation with heavy Xe<sup>22+</sup> ions, depending on the energy of incident particles (the spectra are grouped by dose): a) 10<sup>13</sup> ion/cm<sup>2</sup>; b) 5 × 10<sup>13</sup> ion/cm<sup>2</sup>; c) 10<sup>14</sup> ion/cm<sup>2</sup>.

differences in the transmission value change at doses of  $10^{13}$ – $5 \times 10^{13}$  ion/cm<sup>2</sup>, which vary from 1.2 to 7–12% depending on the ion energy, while for the samples irradiated at a fluence of  $10^{14}$  ion/cm<sup>2</sup>, the average decrease in the transmittance is 10% with an increase in the ion energy.

The established dose and energy dependences of the induced absorption bands formation, as well as changes in the band gap and transmission, made it possible to estimate the change in the electron and optical density of ceramics before and after irradiation.

In the future, dependences obtained can serve to expand the fundamental knowledge about the dynamics of radiation damage in ZrO<sub>2</sub> ceramic, and can also be used as a basis for determination of the service life of these ceramics as optoelectronic devices exposed to radiation effects comparable in energy to uranium fission fragments.

### Credit author statement

Conceptualization - A. Kozlovskiy, M.V. Zdorovets, M.Alin, Uglov V. V. Data curation - A.L. Kozlovskiy, M.Alin, Uglov V.V. Formal analysis - A.L. Kozlovskiy, M.V. Zdorovets. Investigation; Methodology - A.L. Kozlovskiy, M.V. Zdorovets, Koloberdin M.V., Kurakhmedov A.E. Project administration - M.V. Zdorovets. Resources - M.V. Zdorovets. Software - A.L. Kozlovskiy, M.Alin. Supervision - M.V. Zdorovets. Validation - A.L. Kozlovskiy, Visualization - A.L. Kozlovskiy, Ivanov I.A. M.Alin, Sapar A. Roles/Writing - original draft - A.L. Kozlovskiy, Zdorovets. Writing - review & editing - A.L. Kozlovskiy, M.V. Zdorovets, Ivanov I.A.

### Funding

This work was supported by the Grant No. BR09158499 (Development of complex scientific research in the field of nuclear and radiation physics on the basis of Kazakhstan accelerator complexes) of the Ministry of Energy of the Republic of Kazakhstan.

### Ethical approval

This chapter does not contain any studies with human participants or animals performed by any of the authors.

### Informed consent

Informed consent was obtained from all individual participants included in the study.

### Declaration of competing interest

The authors declare that they have no known competing financial interests or personal relationships that could have appeared to influence the work reported in this paper. We have to note that this manuscript is original, and not being or having been submitted for publication to other journals.

### References

- [1] Khalid Mujasam Batoo, et al., Improved room temperature dielectric properties of Gd<sup>3+</sup> and Nb<sup>5+</sup> co-doped Barium Titanate ceramics, *J. Alloys Compd.* (2021) 160836–160856.
- [2] Deo Prakash, C. Amente, K. Dharamvir, B. Singh, R. Singh, E.R. Shaaban, K. D. Verma, Synthesis, purification and microstructural characterization of nickel doped carbon nanotubes for spintronic applications, *Ceram. Int.* 42 (2016) 5600–5606.
- [3] A. Rais, K. Taïbi, A. Addou, A. Zanoun, Y. Al-Douri, Copper substitution effect on the structural properties of nickel ferrites, *Ceram. Int.* 40 (2014) 14413–14419.
- [4] R. Al-Gaashani, S. Radiman, A.R. Daud, N. Tabet, Y.J.C.I. Al-Douri, XPS and optical studies of different morphologies of ZnO nanostructures prepared by microwave methods, *Ceram. Int.* 39 (2013) 2283–2292.
- [5] Y. Al-Douri, K. Gherab, K.M. Batoo, E.H. Raslan, Detecting the DNA of dengue serotype 2 using aluminium nanoparticle doped zinc oxide nanostructure:

- synthesis, analysis and characterization, *Journal of Materials Research and Technology* 9 (2020) 5515–5523.
- [6] A. Bouhemadou, D. Allali, K. Boudiaf, B. Al Qarni, S. Bin-Omran, R. Khenata, Y. Al-Douri, Electronic, optical, elastic, thermoelectric and thermodynamic properties of the spinel oxides ZnRh<sub>2</sub>O<sub>4</sub> and CdRh<sub>2</sub>O<sub>4</sub>, *J. Alloys Compd.* 774 (2019) 299–314.
  - [7] M.E.A. Monir, H. Baltach, A. Abdiche, Y. Al-Douri, R. Khenata, S.B. Omran, C. H. Voon, Doping-induced half-metallic ferromagnetism in vanadium and chromium-doped alkali oxides K<sub>2</sub>O and Rb<sub>2</sub>O: ab initio method, *J. Supercond. Nov. Magnetism* 30 (8) (2017) 2197–2210.
  - [8] A. Bouhemadou, O. Boudrifa, N. Guechi, R. Khenata, Y. Al-Douri, S. Uğur, S. Bin-Omran, Structural, elastic, electronic, chemical bonding and optical properties of Cu-based oxides ACuO (A = Li, Na, K and Rb): an ab initio study, *Comput. Mater. Sci.* 81 (2014) 561–574.
  - [9] Xu, T., Lv, W., Li, Q., Shi, Y., Fang, J., Xia, Z., & Yu, J. "Anti-corrosion Lao<sub>3</sub>/2-GaO<sub>3</sub>/2-ZrO<sub>2</sub> infrared glasses with high refractive index and low dispersion prepared by aerodynamic levitation." *Opt. Mater.* 114 (2021): 110943.
  - [10] M.Z. Naser, Properties and material models for common construction materials at elevated temperatures, *Construct. Build. Mater.* 215 (2019) 192–206.
  - [11] Folke Björk, Tomas Enochsson, Properties of thermal insulation materials during extreme environment changes, *Construct. Build. Mater.* 23 (6) (2009) 2189–2195.
  - [12] Suresh Sagadevan, S. Vennila, A.R. Marlinda, Y. Al-Douri, M.R. Johan, & Lett, J. A. "Synthesis and evaluation of the structural, optical, and antibacterial properties of copper oxide nanoparticles, *Appl. Phys. A* 125 (8) (2019) 489–497.
  - [13] V.C.S. Tony, C.H. Voon, C.C. Lee, B.Y. Lim, S.C.B. Gopinath, K.L. Foo, Y. Al-Douri, Effective synthesis of silicon carbide nanotubes by microwave heating of blended silicon dioxide and multi-walled carbon nanotube, *Materials Research-Ibero-american Journal of Materials* 20 (2017) 1658–1668.
  - [14] Joannie W. Chin, Tihn Nguyen, Aouadi Khaleel, Effects of environmental exposure on fiber-reinforced plastic (FRP) materials used in construction, *J. Compos. Technol. Res.* 19 (4) (1997) 205–213.
  - [15] S.J. Zinkle, E.R. Hodgson, Radiation-induced changes in the physical properties of ceramic materials, *J. Nucl. Mater.* 191 (1992) 58–66.
  - [16] K.K. Kadyrzhanov, K. Tinishbaeva, V.V. Uglov, Investigation of the effect of exposure to heavy Xe<sup>22+</sup> ions on the mechanical properties of carbide ceramics, *Eurasian Phys. Tech. J* 17 (2020) 46–53.
  - [17] M.N. Mirzayev, S.H. Jabarov, E.B. Asgerov, R.N. Mehdiyeva, T.T. Thabethe, S. Biira, N.V. Tjep, Crystal structure changes and weight kinetics of silicon-hexaboride under gamma irradiation dose, *Results in Physics* 10 (2018) 541–545.
  - [18] L.L. Snead, S.J. Zinkle, D.P. White, Thermal conductivity degradation of ceramic materials due to low temperature, low dose neutron irradiation, *J. Nucl. Mater.* 340 (2) (2005) 187–202, 3.
  - [19] Carl E. Johnson, K.R. Kummerer, E. Roth, Ceramic breeder materials, *J. Nucl. Mater.* 155 (1988) 188–201.
  - [20] F. Wang, X. Yan, T. Wang, Y. Wu, L. Shao, M. Nastasi, B. Cui, Irradiation damage in (Zr<sub>0.25</sub>Ta<sub>0.25</sub>Nb<sub>0.25</sub>Ti<sub>0.25</sub>) C high-entropy carbide ceramics, *Acta Mater.* 195 (2020) 739–749.
  - [21] R. Florez, M.L. Crespillo, X. He, T.A. White, G. Hilmis, W. Fahrenholtz, J. Graham, The irradiation response of ZrC ceramics under 10 MeV Au<sup>3+</sup> ion irradiation at 800 °C, *J. Eur. Ceram. Soc.* 40 (5) (2020) 1791–1800.
  - [22] A. Han, H. Ding, J.K.H. Tsoi, S. Imazato, J.P. Matinlinna, Z. Chen, Prolonged UV-C irradiation is a double-edged sword on the zirconia surface, *ACS Omega* 5 (10) (2020) 5126–5133.
  - [23] Vladimir A. Stepanov, Pavel V. Demenkov, Olga V. Nikulina, Radiation hardening and optical properties of materials based on SiO<sub>2</sub>, *Nuclear Energy and Technology* 7 (2021) 145.
  - [24] R. Naik, A. Aparimita, D. Alagarasan, S. Varadharajaperumal, R. Ganesan, Linear and nonlinear optical properties change in Ag/GeS heterostructure thin films by thermal annealing and laser irradiation, *Opt. Quant. Electron.* 52 (3) (2020) 1–18.
  - [25] Y. Yamamoto, N. Ishikawa, F. Hori, A. Iwase, Analysis of ion-irradiation induced lattice expansion and ferromagnetic state in CeO<sub>2</sub> by using Poisson distribution function, *Quantum Beam Science* 4 (3) (2020) 26.
  - [26] M. Lang, F. Djurabekova, N. Medvedev, M. Toulemonde, C. Trautmann, Fundamental Phenomena and Applications of Swift Heavy Ion Irradiations, 2020 arXiv preprint arXiv:2001.03711.
  - [27] R.A. Rymzhanov, N. Medvedev, A.E. Volkov, Damage threshold and structure of swift heavy ion tracks in Al<sub>2</sub>O<sub>3</sub>, *J. Phys. Appl. Phys.* 50 (47) (2017) 475301.
  - [28] R.A. Rymzhanov, N. Medvedev, J.H. o'Connell, A.J. van Vuuren, V.A. Skuratov, A. E. Volkov, "Recrystallization as the governing mechanism of ion track formation, *Sci. Rep.* 9 (1) (2019) 1–10.
  - [29] X. Han, Y. Liu, M.L. Crespillo, E. Zarkadoula, Q. Huang, X. Wang, P. Liu, Latent tracks in ion-irradiated LiTaO<sub>3</sub> crystals: damage morphology characterization and thermal spike analysis, *Crystals* 10 (2020) 877, 10.
  - [30] H.D. Mieskes, W. Assmann, F. Grüner, H. Kucal, Z.G. Wang, M. Toulemonde, Electronic and nuclear thermal spike effects in sputtering of metals with energetic heavy ions, *Phys. Rev. B* 67 (15) (2003) 155414.
  - [31] Z.G. Wang, C. Dufour, S. Euphrasie, M. Toulemonde, Electronic thermal spike effects in intermixing of bilayers induced by swift heavy ions, *Nucl. Instrum. Methods Phys. Res. Sect. B Beam Interact. Mater. Atoms* 209 (2003) 194–199.
  - [32] H. Amekura, M. Toulemonde, K. Narumi, R. Li, A. Chiba, Y. Hirano, Y. Saitoh, Ion tracks in silicon formed by much lower energy deposition than the track formation threshold, *Sci. Rep.* 11 (1) (2021) 1–11.
  - [33] K. Tomić Luketić, M. Karlušić, A. Gajović, S. Fazinić, J.H. O'Connell, B. Pielić, M. Kralj, Investigation of ion irradiation effects in silicon and graphite produced by 23 MeV I beam, *Materials* 14 (8) (2021) 1904.
  - [34] B. Sathyaseelan, E. Manikandan, I. Baskaran, K. Senthilnathan, K. Sivakumar, M. K. Moodley, M. Maaza, Studies on structural and optical properties of ZrO<sub>2</sub>

- nanopowder for opto-electronic applications, *J. Alloys Compd.* 694 (2017) 556–559.
- [35] U. Peuchert, Y. Okano, Y. Menke, S. Reichel, A. Ikesue, Transparent cubic-ZrO<sub>2</sub> ceramics for application as optical lenses, *J. Eur. Ceram. Soc.* 29 (2) (2009) 283–291.
- [36] H. Guo, T.J. Bayer, J. Guo, A. Baker, C.A. Randall, Current progress and perspectives of applying cold sintering process to ZrO<sub>2</sub>-based ceramics, *Scripta Mater.* 136 (2017) 141–148.
- [37] A. Sabur, M.Y. Ali, M.A. Maleque, A.A. Khan, Investigation of material removal characteristics in EDM of nonconductive ZrO<sub>2</sub> ceramic, *Procedia Engineering* 56 (2013) 696–701.
- [38] Floriana-Dana Börner, Wolfgang Lippmann, Antonio Hurtado, Laser-joined Al<sub>2</sub>O<sub>3</sub> and ZrO<sub>2</sub> ceramics for high-temperature applications, *J. Nucl. Mater.* 405 (1) (2010) 1–8.
- [39] P. Chen, Q. Liu, X. Li, Y. Feng, X. Chen, X. Liu, J. Li, Influence of terminal pH value on co-precipitated nanopowders for yttria-stabilized ZrO<sub>2</sub> transparent ceramics, *Opt. Mater.* 98 (2019) 109475.
- [40] X. Hou, S. Zhou, Y. Li, W. Li, Effect of ZrO<sub>2</sub> on the sinterability and spectral properties of (Yb<sub>0.05</sub>Y<sub>0.95</sub>)<sub>2</sub>O<sub>3</sub> transparent ceramic, *Opt. Mater.* 32 (9) (2010) 920–923.
- [41] L. Gan, Y.J. Park, H. Kim, J.M. Kim, J.W. Ko, J.W. Lee, The effects of the temperature and pressure on ZrO<sub>2</sub>-doped transparent yttria ceramics fabricated by a hot-pressing method, *Opt. Mater.* 71 (2017) 109–116.
- [42] S.F. Wang, F. Gu, M.K. Lü, Z.S. Yang, G.J. Zhou, H.P. Zhang, S.M. Wang, Structure evolution and photoluminescence properties of ZrO<sub>2</sub>: Eu<sup>3+</sup> nanocrystals, *Opt. Mater.* 28 (10) (2006) 1222–1226.
- [43] M. Alin, A.L. Kozlovskiy, M.V. Zdorovets, V.V. Uglov, Comprehensive study of changes in the optical, structural and strength properties of ZrO<sub>2</sub> ceramics as a result of phase transformations caused by irradiation with heavy ions, *J. Mater. Sci. Mater. Electron.* (2021) 1–12.
- [44] O.N. Gorshkov, D.O. Filatov, A.P. Kasatkin, V.A. Novikov, D.I. Tetelbaum, S. A. Trushin, M.V. Stepihova, Fabrication of the nanocrystal structures ZrO<sub>2</sub>(y): Zr and SiO<sub>2</sub>: Si (p) by ion implantation, in: *International Workshop on Nondestructive Testing and Computer Simulations in Science and Engineering* vol. 3687, International Society for Optics and Photonics, 1999.
- [45] O.N. Gorshkov, V.A. Novikov, A.P. Kasatkin, Formation of nanoparticles in the surface layer of stabilized ZrO<sub>2</sub> under ion irradiation, *Neorg. Mater.* 35 (5) (1999) 604–610.
- [46] Y. Saito, Y. Imamura, A. Kitahara, Optical properties of YSZ implanted with Ag ions, *Nucl. Instrum. Methods Phys. Res. Sect. B Beam Interact. Mater. Atoms* 206 (2003) 272–276.
- [47] Werner Wesch, Elke Wendler, *Ion Beam Modification of Solids*, vol. 61, Springer Nature, 2016.
- [48] W.J. Weber, D.M. Duffy, L. Thomé, Y. Zhang, The role of electronic energy loss in ion beam modification of materials, *Curr. Opin. Solid State Mater. Sci.* 19 (1) (2015) 1–11.
- [49] A.L. Kozlovskiy, M.V. Zdorovets, Study of the radiation disordering mechanisms of AlN ceramic structure as a result of helium swelling, *J. Mater. Sci. Mater. Electron.* (2021) 1–12.
- [50] A.Z. Tuleushev, F.E. Harrison, A.L. Kozlovskiy, M.V. Zdorovets, Induced spirals in polyethylene terephthalate films irradiated with Ar ions with an energy of 70 MeV, *Crystals* 10 (6) (2020) 427.
- [51] A.Z. Tuleushev, F.E. Harrison, A.L. Kozlovskiy, M.V. Zdorovets, Assessment of the irradiation exposure of PET film with swift heavy ions using the interference-free transmission UV-vis transmission spectra, *Polymers* 13 (3) (2021) 358.